Radio jets as decelerating relativistic flows

R.A. Laing (ESO), A.H. Bridle (NRAO), J.R. Canvin (U. Sydney)

1 Introduction

The largest-scale manifestation of Special Relativistic aberration [3] in contemporary astrophysics is the appearance of initial asymmetries in kpc-scale radio-galaxy jets. This is an effect of aberration on radiation from intrinsically symmetrical, bulk-relativistic outflows. It is well known that such jets appear one-sided as a result of Doppler beaming, with a jet/counter-jet ratio:

$$I_j/I_{cj} = [(1+\beta\cos\theta)/(1-\beta\cos\theta)]^{2+\alpha}$$

where $\beta = v/c$, θ is the angle to the line of sight and α is the spectral index. But the synchrotron emission from jets is highly polarized, and Special Relativity also modifies the observed linear polarization. Aberration acts differently on radiation from the approaching and receding jets, so their observed synchrotron images represent two-dimensional projections of the magnetic-field structure viewed from different directions θ'_j and θ'_{cj} in the rest frame of the flow:

$$\sin\theta'_j = \sin\theta[\Gamma(1-\beta\cos\theta)]^{-1}$$
$$\sin\theta'_{cj} = \sin\theta[\Gamma(1+\beta\cos\theta)]^{-1}$$

where $\Gamma = (1-\beta^2)^{-1/2}$. This is the key to breaking the degeneracy between β and θ and estimating the physical parameters of the jets.

We model jets in low-luminosity, FR I extragalactic radio sources [2] as intrinsically symmetrical, axisymmetric, relativistic, stationary flows, in which the magnetic fields are assumed to be disordered, but anisotropic. We adopt simple, parameterized functional forms for the geometry and the spatial variations of velocity (allowing both deceleration and transverse gradients), emissivity and field-component ratios. We then optimize the model parameters by fitting to deep VLA images in Stokes I, Q and U. The model brightness distributions are derived by integration along the line of sight, including the effects of anisotropy in the rest-frame emission, aberration and beaming. The model and observed images, described in detail in refs. [1, 4, 5], are compared in the next panel.

2 Comparison between models and data

The asymmetry in total intensity close to the nucleus is characteristic of FR I radio jets [8]. It is correlated with an asymmetry in linear polarization: the apparent magnetic field is *longitudinal* on-axis in the bright bases, but *transverse* at the corresponding locations in the counter-jets. We attribute the asymmetries in brightness and polarization to the effects of aberration and the decrease of both effects with distance from the nucleus to deceleration of the jet by mass loading.

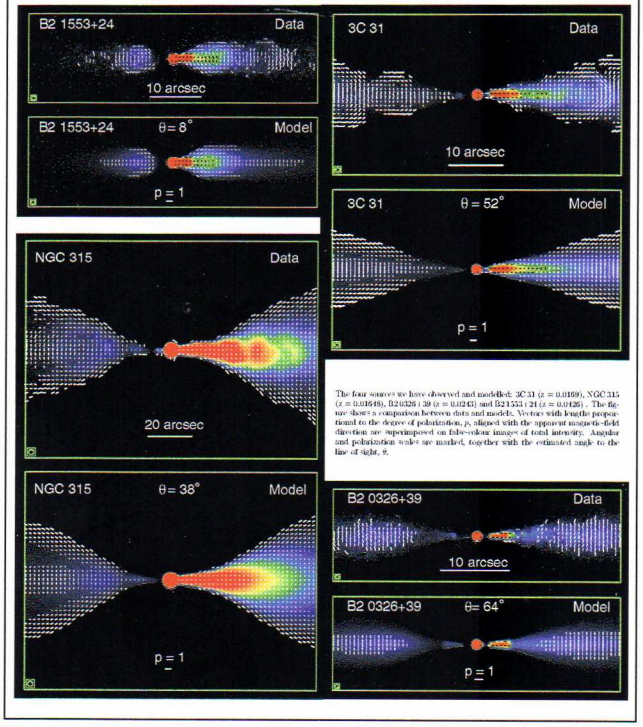

The four sources we have observed and modelled: 3C 31 ($z = 0.0169$), NGC 315 ($z = 0.0146$), B2 0326+39 ($z = 0.0245$) and B2 1553+24 ($z = 0.0126$). The figure shows a comparison between data and models. Vectors with length proportional to the degree of polarization, p, aligned with the apparent magnetic-field direction are superimposed on false-colour images of total intensity. Angular and polarization scales are marked, together with the estimated angle to the line of sight, θ.

3 Key results

1. An intrinsically symmetrical, relativistic jet model provides an excellent description of the total intensity and linear polarization observed in the four sources studied so far and we can use it to estimate the angle to the line of sight and the three-dimensional distributions of velocity, emissivity and magnetic-field structure.
2. The jets in all of the sources decelerate from $\beta \approx 0.8$ to $\beta \approx 0.1 - 0.4$ over short distances within the region of rapid expansion. Further out they recollimate and subsequent deceleration is slower or completely absent. The ratio of edge to on-axis velocity is typically $\approx$0.7.
3. The jets are intrinsically centre-brightened. Their longitudinal emissivity profiles can be modelled as power laws with slopes that flatten with distance.
4. The magnetic field evolves from predominantly longitudinal close to the nucleus to mainly toroidal at large distances; the behaviour of the (weaker) radial component differs between the sources.

4 Velocity and magnetic-field structure

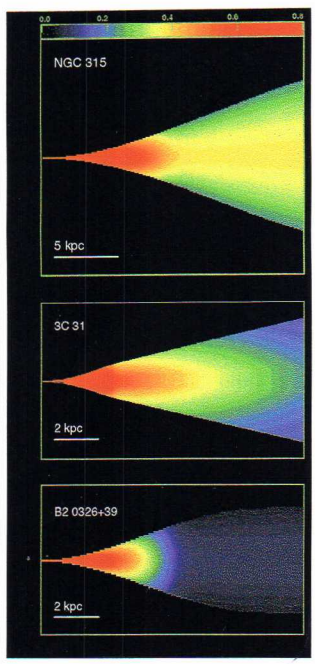

The velocity fields inferred for NGC315, 3C31 and B20326+39. All of the sources have $\beta \approx 0.8$ – 0.9 where they first brighten, decelerate rapidly in the region of rapid expansion to $\beta \approx 0.1$ – 0.4 and then either maintain a constant velocity (NGC315, B20326+39) or decelerate more slowly (3C31). The flow is always faster on-axis, with a typical centre/edge velocity ratio $\approx$0.7.

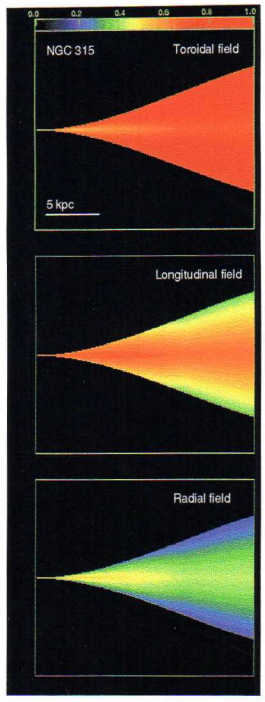

The fractional field components for NGC315, $\langle B_t^2\rangle^{1/2}/B$ (toroidal), $\langle B_l^2\rangle^{1/2}/B$ (longitudinal) and $\langle B_r^2\rangle^{1/2}/B$ (radial), where $B = \langle B_t^2 + B_l^2 + B_r^2\rangle^{1/2}$ is the mean total field. The relative strength of the toroidal field component increases with distance, qualitatively but not quantitatively as expected from flux freezing in an expanding flow.

Note that we assume that the field is disordered on small scales, but anisotropic. Our results would be unchanged if the toroidal component is vector-ordered but we can rule out a helical field [4].

5 Conservation law analysis

Given a kinematic model derived from the radio data alone and a knowledge of the external density and pressure from X-ray observations, we can apply the laws of conservation of mass, momentum and energy for a bulk relativistic flow to estimate the variation of dynamical quantities along the jets [6]. We need to make two additional assumptions to close the problem: the jets are in pressure balance with the external medium at large distances and the ratio of their energy and momentum fluxes on small scales is c. The full lines show the internal flow variables; the external (dashed) and synchrotron minimum (dotted) pressures are also plotted. The density ratio η between the jets and the surrounding medium is very low ($\eta \approx 10^{-5} - 10^{-4}$) and both jets are transonic. The main differences are that the jets in NGC 315 are less dense and have a much lower mass flux. We attribute the differences to the gaseous environments: 3C 31 has a dense group gas component, whereas NGC 315 does not.

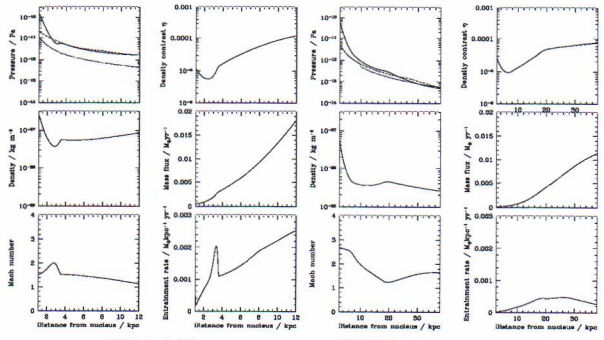

3C 31 (ref. [6]) NGC 315 (Laing et al., in preparation)

[1] Canvin J.R., Laing R.A., 2004, MNRAS, 350, 1342
[2] Fanaroff B.L., Riley J.M., 1974, MNRAS, 167, 31P
[3] Einstein, A., 1905, Annalen der Physik, 17, 140
[4] Canvin J.R., Laing R.A., Bridle A.H., Cotton W.D., 2005, MNRAS, in press (astro-ph/0508440)
[5] Laing R.A., Bridle A.H., 2002a, MNRAS, 336, 328
[6] Laing R.A., Bridle A.H., 2002b, MNRAS, 336, 1161
[7] Laing R.A., Bridle A.H., 2004, MNRAS, 348, 1459
[8] Laing R.A., Parma P., de Ruiter H.R., Fanti, R., 1999, MNRAS, 306, 513